RSC Advances

Comparison of Synergistic Effect of Counterions on Corrosion Inhibition of Mild Steel in Acid Solution: Electrochemical, Gravimetric and Thermodynamic Studies

Journal:	*RSC Advances*
Manuscript ID:	RA-ART-10-2014-012286.R1
Article Type:	Paper
Date Submitted by the Author:	28-Nov-2014
Complete List of Authors:	Wang, Hong-Yan; School of Chemistry and Chemical Engineering, Bai, Li; School of Materials Science and Engineering, Xi'an University of Technology, Feng, Lajun; Xi'an University of Technology, School of Materials Science and Engineering Lu, Yong-Bin; Research Institute of Yanchang Petroleum (Group) CO. LTD, LEI, XIAO-WEI; State Key Laboratory for Mechanical Behavior of Materials, Xi'an Jiaotong University,, BAI, FANG-LIN; Research Institute of Yanchang Petroleum,

RSC Advances

Dynamic Article Links ▶

Cite this: DOI: 10.1039/c0xx00000x

www.rsc.org/xxxxxx

ARTICLE TYPE

Comparison of Synergistic Effect of Counterions on Corrosion Inhibition of Mild Steel in Acid Solution: Electrochemical, Gravimetric and Thermodynamic Studies

Li Bai[a], La-Jun Feng[a], Hong-Yan Wang[b*], Yong-Bin Lu[c], Xiao-Wei Lei[d], Fang-Lin Bai[c]

Received (in XXX, XXX) Xth XXXXXXXXX 20XX, Accepted Xth XXXXXXXXX 20XX
DOI: 10.1039/b000000x

Quinoline quaternary ammonium salts 1-benzylquinoline bromide (**1**) and 1-benzylquinoline chloride (**2**) have been synthesized and then developed as corrosion inhibitors in acidic HCl solution. Electrochemical impedance, potentiodynamic polarization, gravimetric measurements and SEM indicate both of them can efficiently protect the mild steel from corrosion. Under the same condition, the fact that better performance of **1** than **2** should be assigned to the cooperative effect of counterions on corrosion behavior. Thermodynamic and electrochemical studies in agreement with the observed inhibition efficiency announce counterions can affect interaction between organic cations and metal surface, influence the stability of protection film, which leads to the detective differences in inhibition behavior.

1. Introduction

Iron-containing mild steel has been widely employed in petroleum industry and machinery. Due to the prevalent application of acidic solution in oil well acidification and enhanced oil recovery techniques, the severe corrosion of materials causes the serious problems in economics and safety.[1] It is generally acknowledged that organic inhibitor represents an important and practical category for metals prevention from corrosion, coating on the metal surface as a physical barrier to restrict the exposure of steel to acid medium.[2-4] Up to now, various organic compounds are reported as effective, inexpensive and less polluting corrosion inhibitors for mild steel in acid medium. Typically, N-heterocyclic inhibitors act by adsorption on the metal surface, via filling electrons into metal from nitrogen heteroatoms, triple or conjugated double bonds as well as aromatic rings in their molecular structures.[5-9] In some recent published literature, quinoline and its derivatives have been highlighted as useful inhibitors.[10-12] Among them, quaternary ammonium salt can act as prevailing organic inhibitor to achieve excellent inhibition effect based on the predominant water-solubility.[13-15]

As regard to the corrosion efficiency, synergistic effect demonstrates an effective method to improve the inhibitive action of an inhibitor in the presence of another species in corrosive medium. Typically, the synergism between organic compounds and halides salts (eg. NaX) added into the inhibitive solution has been paid wide attention to.[16-22] It is usually considered that the halide irons can create oriented dipoles to change the charge on corroding electrode surface, accordingly facilitates the absorption of inhibitor cations.[23] The existing data in the most cases indicate that the synergism effect of the halide ions is found in the order I^- >Br^->Cl^-.[16-22] Jeyaprabha explained that the cooperative effect of ions depends on their absorption with metal surface.[24] Besides, the synergistic effect of halides salts on improving corrosion inhibition behavior of quaternary ammonium salts is also well documented.[14,25,26] The results highlights the important features of the additives which determine interaction between the inhibitor and the metallic surface to some extent. Since halides salts can synergistically affect the interaction between the inhibitor and the metallic surface, whether and how counterions in inhibitors influence the absorption of organic inhibitors, and leads to the detective effect on inhibition has not been received a considerable amount of attention. Meanwhile, the corresponding mechanism is still unclear. If it can be explained theoretically, changing counterion in inhibitors can be another useful application to produce efficient inhibitors without complicated synthesis.

Considering above in mind, we will present two kinds of quinoline quaternary ammonium salts 1-benzylquinoline bromide (**1**) and 1-benzylquinoline chloride (**2**) synthesized by quaternization of quinoline and benzyl bromide or benzyl chloride respectively, and developed as corrosion inhibitors in acidic HCl solution. Better corrosion inhibition performance displayed in the presence of **1** highlights the cooperative effect of counterions on corrosion behavior. Here, in the combination electrochemistry with thermodynamic studies, it is hopeful to afford persuasive evidences to shed light on the happenings at the metal surface. Our findings on the cooperative effect of

counterions indicate that counterions can affect the interaction between organic cations and metal surface, influence the stability of protection film, lead to the different inhibition results.

2. Experimental method

2.1. Materials and Instrumentation

All reactions and operations were carried out under a dry N_2 atmosphere with standard Schlenk techniques. All solvents were used directly without further dryness and distillation. Quinoline, benzyl bromide and benzyl chloride were purchased from Aldrich and used as received. ^{1}H NMR spectra were run on a Bruker-400 spectrometer with tetramethylsilane (^{1}H) as an internal standard. Mass spectra were recorded with Trio-2000 GC–MS spectrometers.

2.2. Synthesis and characterization

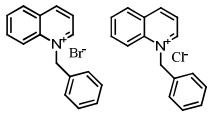

1 2

Fig. 1 The structure of **1** and **2**

The structure of **1** and **2** are shown in **Fig. 1**. The synthesis of compounds **1** and **2** were prepared according to the general procedures known from the literature,[27,28] except that ethanol was used as the solvent instead. Keeping the ratio between quinoline and benzyl bromide of 1 to 1.1 should be the best condition for the synthesis of **1**. However, for **2**, 1mol quinoline reacted with 1.3-1.5 mol benzene chloride, otherwise sticky and dark red by-product was obtained instead. The mixture was refluxed until the reagents had completely reacted, as monitored by TLC (SiO_2; $CH_3COOC_2H_5/CH_2Cl_2$, 30:70 v/v). The color of the reaction changed into dark red, and the obtained precipitation was filtered and collected. The crude products were purified by flash column chromatography with $CH_3COOC_2H_5/CH_2Cl_2$ as eluent. Removal of solvent can afford pink powder. After the powder was dissolved into CH_2Cl_2, the solution was poured into diethyl ether, and white precipitations were collected by filtration, then washed with ethanol three times. The pure products of **1** and **2** were lily-white powder.

1: ^{1}H NMR (D_2O, 400 MHz) δ: 9.31 (d, J = 5.6 Hz, 1H), 9.14 (d, J = 8 Hz, 1H), 8.32 (d, J = 8.4 Hz, 2H), 8.07 (m, 2H), 7.91 (m, 1H), 7.39 (m, 3H), 7.29 (m, 2H), 6.24 (s, 2H); ESI-MS: *m/z* = 220.1 (M^+);

2: ^{1}H NMR (D_2O, 400 MHz) δ: 9.31 (d, J = 5.6 Hz, 1H), 9.13 (d, J = 8 Hz, 1H), 8.31 (d, J = 8.4 Hz, 2H), 8.06 (d, J = 5.2 Hz, 2H), 7.91 (m, 1H), 7.39 (m, 3H), 7.30 (m,2H), 6.24 (s, 2H); ESI-MS: *m/z* = 220.1 (M^+).

2.3 Corrosion tests performed in acidic medium

2.3.1 Specimens and preparations of acidic solution

The specimens were the usual mild steel which were widely used in the oil gas and industry. The chemical composition of the test material is listed in Table **1**, which is analyzed using the direct reading spectrometer (Baird Spectrovac 2000) on the basis of GB/T 4336-2002. In order to ensure the reproducibility, three parallel specimens were tested during the experiments. Besides, here, a solution of 1.0 M HCl prepared from concentrated HCl (37%) (Merck grade) is used as acidic medium to check the activity of tested inhibitors

2.3.2 Electrochemical measurements

Electrochemical experiments were carried out in a conventional three-electrode cell with a platinum counter electrode (CE) and a saturated calomel electrode (SCE, saturated KCl aqueous solution) coupled to a fine Luggin capillary as the reference electrode. To minimize the ohmic contribution, the Luggin capillary was kept close to the working electrode. The working electrode (WE) is in the form of the tested steel embedded in PVC holder using epoxy resin leaving one surface of area 1.0 cm×1.0 cm exposed. The exposed surface was abraded with emery paper up to $^{\#}$800 progressively, then degreased with acetone, rinsed with absolute alcohol and dried with a cold air stream. Before measurement, the electrode was immersed in 1.0 M HCl solution with different inhibitor concentrations at open circuit potential (OCP) at 25 $^{\circ}$C for 2 h to be sufficient to attain a stable state. All electrochemical measurements were carried out using CS350 advanced electrochemical system (Princeton Applied Research). Each experiment was repeated at least three times to check the reproducibility, and acceptable reproducibility was obtained.

The potential of potentiodyamic polarization curves was conducted ranging from -100 mV to +100 mV versus OCP with a scan rate of 0.5 mV s^{-1}. Current response was recorded and analyzed as Tafel plots. Corrosion characteristics such as corrosion potential (E_{corr}), corrosion current (I_{corr}) and anodic (β_a)/cathodic (β_c) Tafel slopes were obtained from the software installed in the instruments. Inhibition efficiency (η_P) was defined and calculated from I_{corr} values as follows:[29]

$$\eta_P = \frac{(I_{corr} - I_{corr(inh)})}{I_{corr}} \times 100 \quad (1)$$

where I_{corr} and $I_{corr(inh)}$ represent the corrosion current density without and with inhibitor, respectively.

Electrochemical impedance spectroscopy (EIS) was carried out at OCP in the frequency range of 100 kHz to 10 mHz using a 10 mV peak-to-peak voltage excitation. The impedance data were fitted using Zview software. The Inhibition efficiency (η_i) is determined on the basis of the equation:[29]

$$\eta_i = \frac{(R_{t(inh)} - R_{t(0)})}{R_{t(inh)}} \times 100 \quad (2)$$

where $R_{t(0)}$ and $R_{t(inh)}$ are charge transfer resistance for mild steel in the absence and presence of inhibitor, respectively.

2.3.3 Weight loss tests

The surface of specimens with the size of 40 mm × 10 mm × 3 mm used for weight loss tests were mechanically grounded by emery paper up to $^{\#}$800 progressively, then degreased with acetone, rinsed with absolute alcohol, and weighted with a balance (a precision of 0.1 mg), finally mounted in the acid

Table 1 The chemical composition of the test material (wt.%)

Elements	*C*	*Si*	*Mn*	*P*	*S*	*Cr*	*Mo*	*Ni*	*Ti*	*Cu*
Components	0.27	0.26	1.41	0.014	0.003	0.089	0.080	0.049	0.036	0.030

solution. Inhibition efficiencies of the synthesized derivatives were tested at 5.0×10^{-5} M, 1.0×10^{-4} M, 2.0×10^{-4} M and 5.0×10^{-4} M respectively in 500 ml of 1.0 M HCl solution. The treatment solution was poured into sealed glass bottles, then the specimens were suspended into these solutions without stirring and kept at 60 °C, 75 °C, 90 °C respectively for 4 h. Control tests were done in the same way without inhibitors. After the corrosion test, the corroded specimens were wiped with paper tissues, and the scale were gently and carefully cleaned, rinsed with water then absolute alcohol, dried in natural state, and weighed again with the balance (a precise of 0.1 mg) to calculate corrosion rate.

Corrosion rates (k) and inhibitor effectiveness (η_w) are calculated by means of the following equations:[30]

$$k = \frac{(W_0 - W_1)}{At} \times 100 \quad (3)$$

$$\eta_w = \frac{\left(k_{(0)} - k_{(inh)}\right)}{k_{(0)}} \times 100 \quad (4)$$

where k is in $g/m^2 \cdot h$; A is the specimen area (in m^2); W_0 is original weight of the specimen, and W_1 is specimen weight (in g) after the immersion period, t is the immersion period (in h), and $k_{(0)}$ and $k_{(inh)}$ are the corrosion rates without and with an inhibitor, respectively.

2.3.4 SEM and XPS measurements

SEM (Philips XL-20) was utilized to investigate micromorphology of the corrosion scale and XPS (Kratos AXIS ULTRA) was used to check Br^- and Cl^- on the surface. Before SEM observation, the samples were cleaned with acetone in order to remove the surface contamination.

3. Result and discussion

3.1 Potentiodynamic polarization studies

The inhibition mechanism was well known for the competitive substitution of water coating on the surface by inhibitor molecules.[31] Nucleophile centers with heteroatoms and unlocalized π-electron in **1** and **2** are readily available for sharing and donating electron to empty orbit of electrophilic metal to form a coordinate covalent chemical bond. Besides, water solubility of **1** and **2** can enhance substitution with water molecule.

The evaluation of inhibitors **1** and **2** in 1.0 M HCl solution was carried out using potentiodynamic polarization technique. The results are simultaneously related to the effect of inhibitors concentration on both anodic and cathodic curves of mild steel (**Fig. 2**). The electrochemical corrosion parameters such as the free corrosion potential (E_{corr}), corrosion current density (I_{corr}), slope of the cathodic branch (β_c) and slope of the anodic branch (β_a) associated with different conditions were determined and listed in **Table S1**. As reflected from the plots, the presence of the inhibitors **1** or **2** causes a visible decrease in the corrosion rate. The distinct feature is that the Tafel curves bodily shift both the cathodic and anodic processes to lower currents but with different extents, respectively relative to the blank curve. Therefore, **1** and **2** can affect both anodic dissolution of the metal and cathodic evolution of hydrogen to some extent.[32] Compared with the blank experiment, cathodic branches of the polarization curves recorded for both two compounds are shifted more significantly to the direction of the current deduction, in line with higher β_c values.[33] Besides, the values of corrosion potential displace to more positive direction with addition of each compound. Meanwhile, with the increasing concentration of inhibitors, the cathodic Tafel slope (β_c) slightly changes and is approximately independent on the inhibitors concentration. This phenomenon indicates that the addition of **1** and **2** do not change the mechanism of cathodic reactions, and the corrosion is rather inhibited by blocking of the iron surface by simple adsorption process.[34] For anodic dissolution reaction of the metal, during the scanned region, the anodic branches reveal clear inhibited region, just unclear trend for flat region associated with the increasing concentration of inhibitors, suggesting that the inhibitors can efficiently form the protective adsorption film and retard the anodic dissolution reaction.

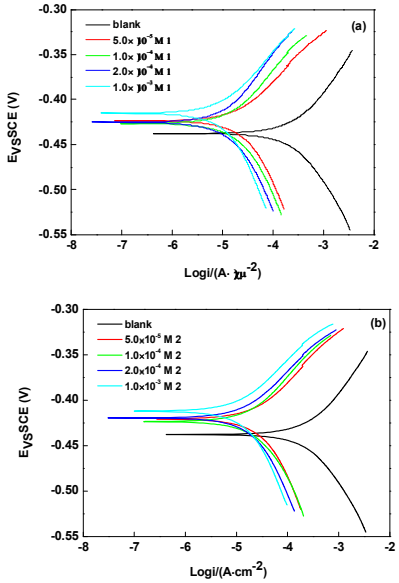

Fig. 2 Effect of **1** (a) and **2** (b) on the polarization behavior of mild steel in 1.0 M HCl at 25 °C respectively

Furthermore, the polarization curves at different concentrations of inhibitors were used to determine the protection efficiency (η_p). The data collected in **Table S1** demonstrates the dependence of η_p on the concentration of the inhibitor. Generally, the inhibition efficiency increases with the inhibitor concentration both in the case of **1** and **2**. The increase in η_p at higher concentrations is not as much as at the low concentration of the inhibitor. For instance, η_p can increase from 0 to 93.11% in the presence of 2.0×10^{-4} M **1**, while the addition of **1** to 1.0×10^{-3} M can simply allow the value of η_p to reach up to 94.47%. This means that the dynamic balance between adsorption and desorption of the inhibitor results in the approximately saturated coverage of molecule, so that higher concentration of inhibitor can not lead to much greater protection

efficiency.[35] The potentiodynamic polarization curves of **1** and **2** shown in **Fig. 2** displayed similar cathodic and anodic lines, indicating the same inhibition mechanism. However, carefully observing the data in **Table S1**, it is not difficult to find out that at each case, the decrease of I_{corr} is more distinct in the presence of **1** compared to **2** under the same condition, implying a better protection.

3.2. Electrochemical impedance spectroscopy (EIS)

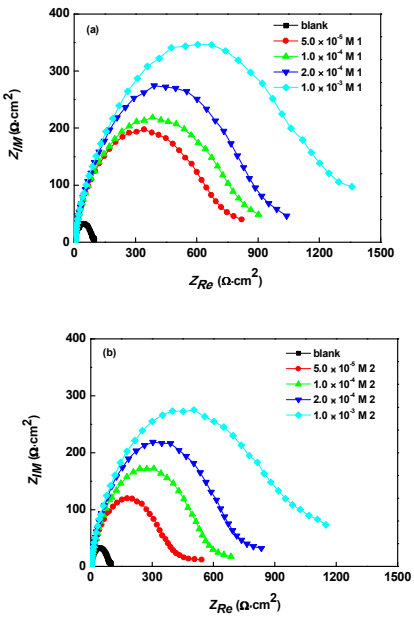

Fig. 3 EIS behavior of mild steel containing different concentrations of **1** (a) and **2** (b) in 1.0 M HCl at 25 °C respectively

Nyquist diagrams for the mild steel in 1.0 M HCl at 25 °C with **1** and **2** were examined by electrochemical impedance spectroscopy respectively, which are shown in **Fig. 3**. Clearly, for both **1** and **2**, every impedance spectra mainly consist of large capacitive loop at high frequencies. The large capacitive loop indicates that the corrosion of the test steel in HCl solution is mainly controlled by charge transfer process and formation of a protective layer on the metal surface. Deviations from the ideal semicircle are generally attributed to the frequency dispersion as well as inhomogeneities, roughness of metal surface and mass transport process.[36-38] Evidently, throughout all tested concentrations, the diameter of the capacitive loop with addition of inhibitors **1** or **2** is bigger than that in their absence, and the changes of impedance response are more pronounced with the increasing concentration of inhibitors.[39] Simultaneously, similar shapes maintaines in all the diagrams, indicating that the presence of inhibitors can not affect the corrosion mechanism for the dissolution of mild steel in HCl.[40]

For analysis of impedance spectra, the convincing fitting results of high frequency capacitive loops of compound **1** for an appropriate equivalent circuit are shown in **Fig. S1**, which consists of a parallel combination of a capacitor C_{dl}, and a charge transfer resistor R_t, in series with solution resistor R_s. Similar fitting results were obtained for **2** as well. The pure electric models can verify or rule out mechanistic models and enable the calculation of numerical values corresponding to the physical and/or chemical properties of the electrochemical system under investigation.[41] The proposed circuit allows the identification of both solution resistance and charge transfer resistance. The capacitance value is affected by imperfections of the surface, which can be simulated via a constant phase element (CPE).[42] The CPE is determined by a component Q_{dl} and a coefficient α, where α quantifies different physical phenomena like surface inhomogeneousness resulting from surface roughness, inhibitor adsorption, porous layer formation, etc. In this case, the capacitance is proposed by the following mathematical formulation:[43]

$$C_{dl} = Q_{dl} \times (2\pi f_{max})^{\alpha-1} \quad (5)$$

where f_{max} represents the frequency at which imaginary component of the impedance is maximal on the Nyquist plot. The electrochemical parameters of R_t, C_{dl} and R_s are calculated by software and presented in **Table S2**.

Inspection of data in **Table S2**, the C_{dl} decreases prominently while R_t values increases with the concentration of inhibitors **1** or **2**, suggesting that the inhibitor molecules function by adsorption at the metal/solution interface.[44] A larger charge transfer resistance is associated with a slower corroding system. In contrast, better protection provided by an inhibitor can be associated with a decrease in capacitance of the metal. Typically, at 5.0×10^{-4} M of inhibitors, the presence of **1** gives R_t value of 655.9 Ω·cm^2 and C_{dl} value of 90.612 μF/cm^2, while **2** gives 406.4 Ω·cm^2 and 111.66 μF/cm^2. At any given condition, R_t(**1**) > R_t(**2**), while C_{dl}(**1**) < C_{dl}(**2**), implying the better inhibition of **1** than that of **2**. The values of inhibition efficiency (η_i) were calculated from R_t in the absence and presence of inhibitor. In both cases, generally, η_i increases with the concentration of inhibitor, and follows the order: η_i (**1**)> η_i (**2**), in accordance with the results in potentiodynamic polarization. However, the values are not in perfect agreement with each other might be due to different testing modes.

Furthermore, the electrochemical impedance spectroscopy in the presence of **1** and **2** at 90 °C as well were measured respectively (**Table S3**, **Fig. S4**). At higher temperature, the steel were corroded more seriously, in accordance with much lower Rt values. With the concentration, inhibition efficiency displayed the similar trend to that at room temperature, but **1** still show much better performance than **2** at the same condition.

3.3 Corrosion inhibition by 1 and 2 based on weight loss tests

Concentration dependent experiments of **1** and **2** (0, 5.0×10^{-5} M, 1.0×10^{-4} M, 2.0×10^{-4} M and 5.0×10^{-4} M respectively) in 1.0 M HCl was studied by weight loss method at 60 °C, 75 °C and 90 °C for 4h respectively. In general, temperature plays an important role in acidic corrosion, which seriously affects the formation rate of the corrosion product layer. At low temperature, without inhibitor, though protective layer is hardly to form on the steel surface due to the low deposition rate of corrosion product, lower dissolution rate of the matrix and lower mass transfer rate can lead to the lower corrosion rate. Instead, the presence of inhibitor benefits for the formation of protective film, which efficiently provides better prevention for the metal surface from exposure to acidic medium. With the increasing of temperature, if without inhibitor, owing to the negative temperature gradient of corrosion

product, it quickly deposits onto the surface of metal. However, this process is accompanied by the acceleration of mass transfer and corrosion product layers dissolution, therefore the corrosion product layers finally become looser and porous, which can not supply the matrix with the effective protection, but increase the contacting area of corrosion reactions. In contrast, in the presence of inhibitor, although the acceleration of thermal motion of the inhibitor molecule with the increasing of temperature, leading to the desorption of inhibitor to some extend, the reliable interaction between inhibitor molecule and empty orbits of electrophilic metal guarantees the steady supply of compact and dense film. Therefore, some powerful inhibitors still display high protective effect at high temperature.[45-47] The variation of corrosion rate (k) with concentrations of inhibitors in HCl is as shown in **Fig. S2**(a), (b) and **Table 2** respectively. Clearly, the steel is more rapidly corroded with temperature in the absence of inhibitor. And the corrosion rate decreases while inhibition efficiency (η_w) increases with the inhibitor concentration.

Table 2 Corrosion rate (k) for mild steel as well as corrosion effect (ηw) with different concentration of inhibitor **1** and **2** in 1.0 M HCl at 60 °C, 75 °C, and 90 °C respectively

t (°C)	60				75				90			
	1		2		1		2		1		2	
Concentration of inhibitors	k g/m^2·h	ηw %	k g/m^2·h	ηw %	k g/m^2·h	η_w %	k g/m^2·h	η_w %	k g/m^2·h	η_w %	k g/m^2·h	η_w %
0	8.3824	0	8.3824	0	27.8309	0	27.8309	0	127.6654	0	127.6654	0
5.0×10^{-5}	0.8365	90.02	0.8640	89.69	1.3971	94.98	6.1949	77.74	9.1177	92.86	34.8796	72.68
1.0×10^{-4}	0.5882	92.98	0.6802	91.89	0.9927	96.43	4.3382	84.41	5.3768	95.79	12.0315	90.58
2.0×10^{-4}	0.5299	93.67	0.6250	92.54	0.7353	97.36	3.2721	88.24	4.1452	96.75	7.7621	93.92
5.0×10^{-4}	0.3493	95.83	0.4963	94.08	0.6802	97.56	1.5441	94.45	3.5846	97.19	6.4129	94.97

It is found in the presence of 2.0×10^{-4} M inhibitor, the corrosion rates of the tested specimens were exhibited with the data that the maximum η_w is 93.76 % at 60 °C, 97.36% at 75 °C, 96.75% at 90 °C for **1** and 92.54 % at 60 °C; 88.24% at 75 °C; 93.92% at 90 °C for **2** respectively. Noticeably, when the concentration of inhibitor is less than 1.0×10^{-4} M, k decreases sharply with an increase in concentration, however, a further increase causes no appreciable change in performance. It is considered that the absorption of inhibitors on the metal surface is exothermic process, therefore, after saturated absorption of inhibitors, the excess molecules desorb from the metal surface due to the intermolecular repulsion. Besides, the fact that η_w slightly increases or almost unchanges with temperature is explained from the standpoint of the likely specific interaction between the iron surface and the inhibitor:[48] the increase of η_w with temperature can lead to the change in the nature of the adsorption mode: at lower temperature, the inhibitor is being physically adsorbed, while chemisorption is favoured as temperature increases.[49]

Table **2** affords visible comparison of performance between **1** and **2** as well. Distinctly, at 90 °C, with the addition of 5.0×10^{-4} M inhibitors, corrosion rates of measured materials decreased from 127.6654 g/m^2·h to 3.5846 g/m^2·h, with η_w of 97.19% for **1,** while k to 6.4129 g/m^2·h and η_w of 94.97% for **2** respectively. Clearly, the materials in the presence of **1** are generally corroded more slowly, in line with the result based on electrochemical analysis.

3.4 SEM analysis of tested materials in the presence or absence of 1 and 2 respectively

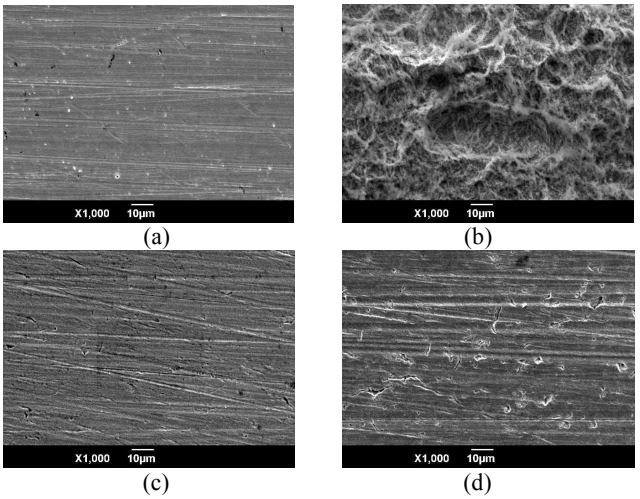

(a) (b) (c) (d)

Fig. 4 SEM of steel surface with: (a) before corrosion; (b) after immersion in 1.0 M HCl, (c) after immersion in 2.0×10^{-4} M **1**, (d) after immersion in 2.0×10^{-4} M **2** at 90 °C for 4h

The effect of inhibitors **1** and **2** on the surface micro-morphology of tested mild steel is explored from SEM images of corroded steel surface in the absence or presence of inhibitors. It can be seen from **Fig. 4**(a) that the steel surface before corrosion shows some abrading scratches. Typically, SEM photographs of resulted surface after immersion in 1.0 M HCl at 90 °C in the absence and presence of 2.0×10^{-4} M **1** or **2** for 4h are shown in **Fig. 4**(b-d) respectively. Close examination of SEM images reveals that the specimen surface was damaged, accompanied by an aggressive attack of the corroding medium on the steel surface. The corrosion scale appears too uneven with the corrosion products arranging layer upon layer. Whereas in the presence of **1** and **2**, the steel displayed smooth surface with a few small notches, means that both two inhibitors can inhibit the dissolution of iron, thereby reduce the rate of corrosion and afford better

protection against corrosion. Less damage of mild steel surface can display with **1** compared to **2**, reveals that **1** facilitates the better protection from acidic corrosion.

Considered molecular structure that the same organic cation but different inorganic anion Br^- or Cl^- can dissociate in aqueous solution from **1** and **2**, the differences in inhibition behavior should be ascribed to the dissociation of quaternary ammonium salts or the effect of the counterions. In general, ^{1}H NMR (Proton Nuclear Magnetic Resonance), a well received method to determine the structure of the organic compounds, can reflect the electronic atmosphere of proton via the interaction between the nuclear and magnetic field. In ^{1}H NMR, no detective differences in **1** and **2** (**Fig S3**), means both **1** and **2** can be completely dissociated in the aqueous solution. Therefore, the influence of halide counterions on corrosion behavior is dominant. It is well known that the corrosion inhibition exhibited by organic molecules is through adsorption on corroding metal. The adsorption is not always a direct combination of organic molecules with the metal surface, but in some case, it takes place via already adsorbed anions in the system.[50,51] Halide ions have been shown to inhibit the corrosion of some metals in strong acids. Inhibition performance depends on ionic size and charge, electrostatic field set up by negative charge of the anion on the adsorption site and the nature of the halide. More stabilization of the adsorbed halide ions by means of interaction with the heterocyclic cation leads to greater surface coverage protection efficiency. The observation in the experiments is in line with the well documented function of halide ions, accordingly the counterion can display cooperative effect on inhibition behavior. Moreover, from the observed differences in the protective action, it can be concluded that if halide ion is treated as conterions induced into inhibitive medium, it still can display a profound influence on the adsorption process.[53-55]

3.5 The effect of temperature and activation parameters of 1 and 2 based on weight loss tests

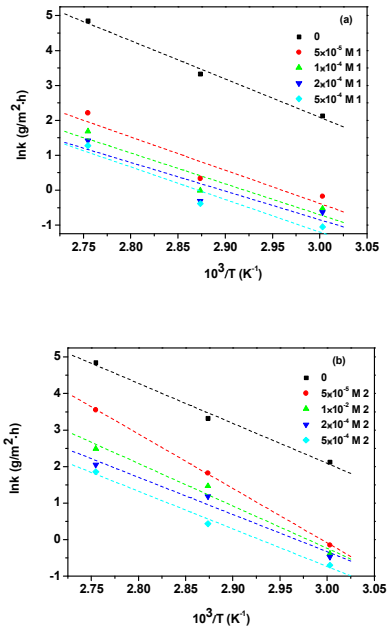

Fig. 5 Arrhenius plots of ln(k) versus 1/T for mild steel in 1.0 M HCl without and with different concentration of the inhibitors **1**(a) and **2**(b) respectively

To further elucidate the inhibition properties, the thermodynamic parameters are very useful to shed light on the absorption behavior of inhibitors. We were interested in exploring the activation energy of the corrosion process of the tested inhibitors, which has been accomplished by investigating the temperature dependence of the corrosion rates. The effect of temperature on the inhibited acid–metal reaction is highly complex, because many changes occur on the metal surface such as rapid etching, desorption of inhibitor and the decomposition and/or rearrangement of inhibitor itself. Based on the study on weight loss measurement, the corrosion rates were found to increase with the temperature for both inhibited and uninhibited acid solutions while they decreased with the increase of inhibitor concentration at a given temperature. It is well known that, temperature dependence effect reflects the activation energy. For the acid corrosion of steel, temperature dependence of the corrosion rate (k) can be expressed by Arrhenius equation, where the natural logarithm of the corrosion rate (k) is a linear function with $\frac{1}{T}$:[56]

$$\ln k = \frac{(-E_a)}{RT} + \ln A \qquad (6)$$

where k is the corrosion rate, E_a is the activation energy, T is the absolute temperature and R is the universal gas constant. Based on gravimetric measurement, **Fig. 5** (a) and (b) graphically represents the regression of ln(k) with the increase of $\frac{1}{T}$ for mild steel in the absence and presence of different concentrations of the synthesized inhibitors **1** and **2** respectively. The straight lines indicate the linear relationship between ln(k) and $\frac{1}{T}$. The E_a

Table 3 Values of activation thermodynamic parameters for mild steel in 1.0 M HCl in the absence and presence of different concentration of the inhibitors **1** and **2** respectively

Concentration M	in the presence of **1**			in the presence of **2**		
	E_a kJ/mol	ΔH^* kJ/mol	ΔS^* kJ/mol·K	E_a kJ/mol	ΔH^* (kJ/mol	ΔS^* kJ/mol·K
0	91.02	-88.09	16.16	91.02	-88.09	16.16
5.0×10^{-5}	79.32	-76.79	-37.24	123.92	-121.04	96.89
1.0×10^{-4}	73.53	-70.61	-59.53	96.58	-93.65	13.49
2.0×10^{-4}	68.20	-65.44	-75.68	84.72	-81.86	-22.67
5.0×10^{-4}	77.48	-74.59	-51.69	85.53	-82.71	-23.48

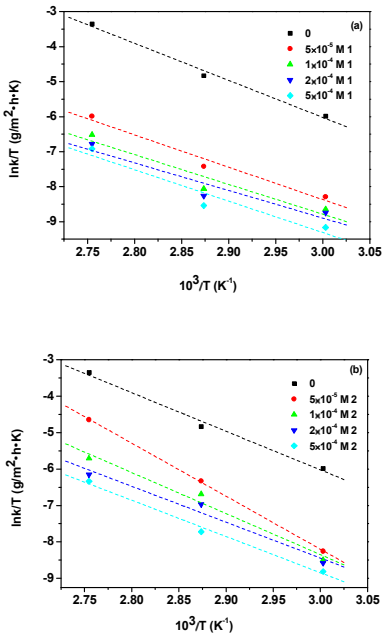

Fig. 6 Arrhenius plots of ln(k/T) versus 1/T for mild steel in 1.0 M HCl without and with different concentration of the inhibitors **1**(a) and **2**(b) respectively

values at different temperature were calculated from the slope, equals to $\frac{-E_a}{R}$ of each straight line, which are listed in Table **3**. Generally, in the presence of **1**, activation energy is lower in the presence of inhibitors than in their absence, and more obvious decrease of the activation energy, is accompanied by more efficient inhibiting effect with the concentration of the synthesized inhibitors. The decrease in E_a with the concentration of **1** is typical of chemisorption. This was attributed by Hoar and Holliday [57] to a slow rate of inhibitor adsorption with a resultant closer approach to equilibrium during the experiments at the higher temperature. But, Riggs and Hurd [58] explained that the decrease in activation energy of corrosion at higher levels of inhibition arises from a shift of the net corrosion reaction from that on the uncovered part on the metal surface to the covered one. Schmid and Huang [59] found that organic molecules inhibit both the anodic and cathodic partial reactions on the electrode surface and a parallel reaction takes place on the covered area, but that the reaction rate on the covered area is substantially less than on the uncovered area. Generally one can say that the nature and the concentration of inhibitor affect greatly the activation energy for the corrosion process. In contrast, with the addition of **2**, the E_a values are increased with the concentration of inhibitor then goes down. This can be interpreted as physical adsorption occurring in the first stage at lower concentration.[60,61] At higher concentration, chemisorption of inhibitors is the prevailing mechanism with the decrease in activation energy, in line with the reported literature: unchanged or lowered activation energy is related to the existence of chemisorption.[58,62-63]

An alternative formulation of the Arrhenius equation is:[64]

$$\ln\left(\frac{k}{T}\right)=\left[\ln\left(\frac{R}{N_A h}\right)+\left(\frac{\Delta S^*}{R}\right)\right]-\frac{\Delta H^*}{RT} \qquad (7)$$

where h is Planck's constant, N_A is Avogadro's number, R is the universal gas constant, ΔH^* is the enthalpy of the activation and ΔS^* is the entropy of activation. Plotting the $\ln\left(\frac{k}{T}\right)$ against $\frac{1}{T}$ gave straight lines with a slope ($\frac{-\Delta H^*}{RT}$) and an intercept of $\ln\left(\frac{R}{N_A h}\right)+\left(\frac{\Delta S^*}{R}\right)$ from which the values of ΔH^* and ΔS^* (shown in Fig. **6**) have been calculated and listed in Table **3**. Inspection of these data, it seemed that E_a and ΔH^* varied in the same fashion.

The presence and absence of inhibitor **1** or **2** does not influence the positive signs of ΔH^*, reflecting that the addition of inhibitors can not affect the corroding nature of the test materials.[65] Besides, the ΔH^* of the dissolution reaction of test steel in 1.0 M HCl in the presence of the inhibitor are generally less than those in their absence. Simultaneously, in the presence of inhibitors, larger and more negative values of entropies ΔS^*, implies that a decrease in disordering takes place on the surface of the mild.[66,67] This might be a result of the adsorption of organic inhibitor molecules from the acidic solution that can be regarded as a quasi-substitution process between the organic compound in the aqueous phase and water molecules at electrode surface.[31] In this situation, the adsorption of organic inhibitor was accompanied by desorption of water molecules from the surface. Compared with inhibitor **1**, although ΔS^* varied from positive to negative values as well with the concentration of **2**, the more slight trend reveals that weaker association between organic molecules and the metal surface, which is in line with the lower inhibition efficiency.

3.6 Thermodynamic parameters of 1 and 2 based on weight loss tests

Table 4 Thermodynamic parameters calculated from Flory-Huggins absorption isotherms for **1** and **2** in 1.0 M HCl at 60 °C, 75 °C and 90 °C respectively

Temperature °C	in the presence of **1**		in the presence of **2**	
	K_{ads} M^{-1}	ΔG^0_{ads} kJ/mol	K_{ads} M^{-1}	ΔG^0_{ads} kJ/mol

60	3.03×10^{6}	-52.44	7.35×10^{6}	-54.89
75	3.33×10^{7}	-61.83	9.09×10^{4}	-44.66
90	3.40×10^{6}	-57.51	1.84×10^{5}	-48.71

Since corrosion of the mild steel is inhibited by the absorption of organic cations, the absorption models should be provided so as to clarify the basic information on the interaction between the inhibitors and the metal surface. The data of the weight loss, obtained by means of directed method, corresponding to different concentrations of **1** or **2** in the 60-90 °C range, are used to study the absorption behavior of inhibitors and to choose the more suitable absorption isotherm. Attempts were made to fit experimental data with various isotherms, such as the Langmuir, Terkin, Frumkin as well as Flory-Huggins isotherms. It is found that Flory-Huggins isotherm is the best description of the adsorption behavior of tested inhibitors, which has the form as follows:[26]

$$\log\left(\frac{\theta}{c}\right) = \log(\chi K_{ads}) + \chi\log(1-\theta) \quad (8)$$

where c is the concentration of inhibitor, K_{ads} the adsorption equilibrium constant, and θ is the surface coverage and expressed by the ration $\frac{\eta_w}{100}$. According to the Flory–Huggins model, plots of $\log\left(\frac{\theta}{c}\right)$ against $\log(1-\theta)$ give straight lines with slope (χ) and intercept $\log(\chi K_{ads})$, shown in Fig. **7**, from which the values of K_{ads} have been calculated and listed in Table **4**. It is generally known that K_{ads} denotes the strength between the adsorbate and adsorbent. Higher K_{ads} values of **1** in line with higher inhibition efficiency evidences the stronger binding power of organic cations on the steel surface, cooperated by Br^-.[68]

Furthermore, the adsorption equilibrium constant (K_{ads}) is related to the standard adsorption free energy (ΔG^0_{ads}) as shown the following equation:[69]

$$-\Delta G^0_{ads} = RT\ln(55.5 K_{ads}) \quad (9)$$

where R is the gas constant, T the absolute temperature, and the value 55.5 is the concentration of water in the solution. The ΔG^0_{ads} values are also presented in Table **4**. Generally, values of ΔG^0_{ads} up to -20 kJ mol^{-1} or less negative are consistent with the electrostatic interaction between the charged molecules and the charged metal (physisorption), while those around -40 kJ mol^{-1} or more negative are assumed for involving sharing or transferring of electrons from the inhibitor molecules to the metal surface to form a coordinate type of bond (chemisorption).[70] The both large negative values of ΔG^0_{ads} in **1** or **2** evidences that the organic species can absorb on the mild steel surface spontaneously with a typical chemisorption, which ensure the absorptive layer is highly stable. In addition, the more negative values in the presence of **1** than that of **2** are as well consistent with the results of the protection efficiency, implying **1** can form a more stable protective film coating on the surface of steel.

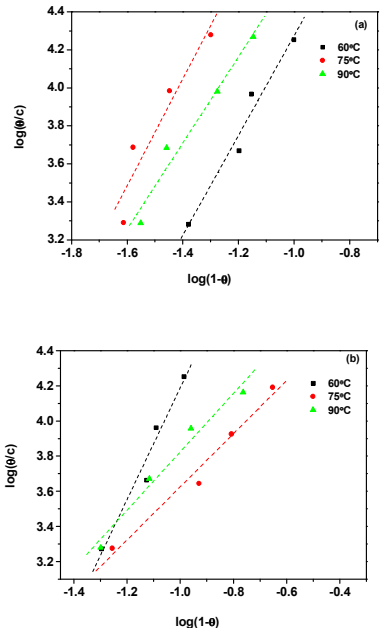

Fig. 7 Flory-Huggins absorption isotherms for **1**(a) and **2**(b) in 1.0 M HCl at 60 °C, 75 °C and 90°C respectively

3.6 Explanation for cooperative effect of cations and mechanism for absorption

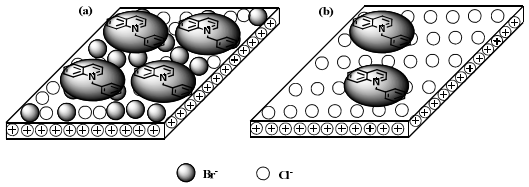

Fig. 8 The proposed mechanism for the inhibition behavior of **1**(a) and **2**(b) respectively

As shown above, apparently, counterions induced into corrosion medium can obviously display cooperative effect on inhibition behavior in the presence of quaternary ammonium salts **1** and **2**. Co-adsorption mechanism is available to interpret the behavior of ionic inhibitor. In fact, co-adsorption mechanism may be either competitive or cooperative adsorption. In competitive adsorption, the anion and the inhibitor cation are adsorbed at different sites on the metal surface. In cooperative adsorption, the anion is absorbed on the metal surface and the cation is adsorbed on a layer of the anion. Sometimes both competitive and cooperative mechanism may occur simultaneously. Based on above results, that cooperative adsorption seems much more dominant. At prime tense, the positively charged mild steel surface prevents organic cations from the metal surface. However, in the presence of HCl, chloride ions can result in the expected specific adsorption, followed by the mild steel surface charged. Being specifically adsorbed, they create an excess negative charge towards the solution and favor the electrostatic adsorption of the cations.[71] Thus, by means of electrostatic attraction, organic cation can access to mild steel solution interface, consequently leading to increasing surface coverage and inhibition efficiency. The following chemical adsorption occurs

by the transfer of electrons from the inhibitor molecules to the unoccupied d-orbital of iron atoms (chemical adsorption) at the mild steel/solution interface.[66] Clearly, the presence of **2** can not lead to the change in the formation of the system but each component. However, the addition of **1** accompanied by the introduction of Br^- ion, can cause that Cl^-, initially adsorbed on anode of metal surface, is displaced by Br^-. This is because Br^- is much more favored to attach on the surface of metal due to the advantage in hydration degree and electro-negativity.[72] Besides, the effect of halide ions depends on the ionic size and charge, the electrostatic field set up by the negative charge of the anion on the adsorption site and the nature and concentration of the halide ion.[46,52] The observed trend of increase in the protective action is in the order $Br^- > Cl^-$, because electronegativity (Br^- = 2.8, Cl^- = 3.0) results in lower repulsion between ions, which helps Br^- is more predisposed to adsorption than chloride ions.[73] Being specially absorbed, bromide can create a more excess negative charge toward solution and allow more organic cations absorption by coulombic attraction, thus leads to more dense film and better protection of steel from exposure to the acidic medium (**Fig. 8**). Additionally, the composition of steel surface after corrosion with inhibitors **1** and **2** was investigated by energy-dispersive X-ray (EDX) spectroscopy. In an EDX spectrum, each element present gives a unique set of peaks and the intensities of these peaks can be used to determine the ratio of the elements in the sample. As shown in **Fig. S5**, the presence of C and N confirms that the corrosion inhibitors can cover on the surface of steel, as protective film to prevent the acid corrosion. X-ray photoelectron spectroscopy (XPS) is a rather surface sensitive method to deduce more detailed information on the surface, which was as well employed to obtain the direct information on the effect of the conterion. A signal around 198-202 eV ascribed to Cl $2p_{1/2}$ and Cl $2p_{3/2}$ shown in **Fig. 9**, confirms in the presence of HCl, chloride ions can result in the expected specific adsorption on the steel surface both with the addition of **1** and **2**.[74] More interestingly, the signal at 69 eV matching the binding energy of Br $3d_{3/2}$ mixed with Br $3d_{5/2}$ indicates the presence of Br^- after the immersion of steel in the HCl solution containing **1**, however, in the same region,[74] there was not detective signals with the addition of **2**. Therefore, it can be implied that the counterion Br^- in **1** can absorb on the steel surface and display a co-adsorption effect between counterions and the organic cations.

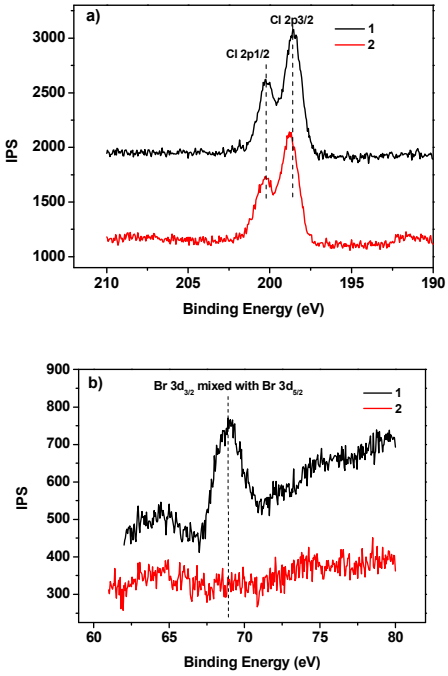

Fig. 9 the XPS fine scans showing the Cl 2p and Br 3d region of steel surface with: 2.0×10^{-4} M **1** (a) and **2** (b) after immersion at 90 °C for 4h

4. Conclusions

Two kinds of quinoline quaternary ammonium salts **1** and **2**, have been synthesized and characterized. Several methods have been employed to evaluate and compare the effectiveness of **1** and **2** under the same condition. The detective differences in inhibition behavior highlight the cooperative effect of counterions. Several interesting results are summarized as fellows:

1) Combined with the potentiodynamic polarization tests, electrochemical impedance, and gravimetric measurements and SEM, both two inhibitors **1** and **2** displayed good inhibition effect on mild steel in HCl acidic solution, but better performance was observed in the presence of **1**;

2) Higher inhibition efficiency of **1** compared to **2** displayed under the same condition highlights counterion can display synergistic effect on inhibiton behavior;

3) The fact that thermodynamic parameters and activation parameters are in agreement with the observed inhibition efficiency evidences that counterions can affect the interaction between organic cations and metal surface as well as the stability of protection film.

4) The counterions can synergistically improve inhibition performance of the inhibitor, in the order of $Br^- > Cl^-$, which can be explained by co-adsorption effect between counterions and the organic cations.

Acknowledgements

The Applied Basic Research Funds (2011D-4603-0102, 2011A-4208) of China National Petroleum Corporation (CNPC), National Support Fund (2011BAE25B04) are gratefully acknowledged.

Notes and references

[a] *School of Materials Science and Engineering, Xi'an University of Technology, Xi'an 710048, P.R. China*
[b] *School of Chemistry and Chemical Engineering, Shaanxi Normol University, Xi'an 710119, P. R. China*
[c] *Research Institute of Yanchang Petroleum (Group) CO. LTD, Xi'an 710075, P.R. China*
[d] *State Key Laboratory for Mechanical Behavior of Materials, Xi'an Jiaotong University, Xi'an 710049, P.R. China*
Corresponding author. Tel.: +46 0729428391.
E-mail address: hongyan-wang@snnu.edu.cn (H. Y. Wang).

† Electronic Supplementary Information (ESI) available: [electrical equivalent circuit used for modeling metal/solution interface; variation of corrosion rate for mild steel with different concentration of inhibitor; ^{1}H NMR spectrum of **1** and **2**; electrochemical parameters from Tafel polarization curves; EIS parameters for corrosion of mild steel with different concentration of inhibitors; EDX and XPS spectrum of the surface with addition of **1** or **2**]. See DOI: 10.1039/b000000x/

Reference

1 R. A. Prabhu, T. V. Venkatesha and A. V. Shanbhag: *Mater. Chem. Phys.*, 2008, **108**, 283-289.
2 H. H. Uhlig, and R.W. Revie: *Corrosion and corrosion Control*, Wiely: New York, 1985.
3 G. Trabanelli: *Corrosion*, 1991, **47**, 410-419.
4 V. S. Sastri: John Wiely and Sons: New York, 1998.
5 J. Aljourani, K. Raeissi, and M. A. Golozar: *Corros. Sci.*, 2009, **51**, 1836–1843.
6 M. L. Zheludkevich, K. A. Yasakau and S. K. Poznyak: *Corros. Sci.*, 2005, **47**, 3368-3383.
7 I. B. Obot, N. O. Obi-Egbedi, and S.A. Umoren: *Corros. Sci.*, 2009, **51**, 276-282.
8 F. Bentiss, M. Bouanis and B. Mernari: *J. Appl. Electrochem.*, 2002, **32**, 671-678.
9 Q. Qu, S. Jiang and W. Bai: *Electrochim. Acta*, 2007, **52**, 6811-6820.
10 S. M. Li, H. R. Zhang, and J. H. Liu: *Trans. Nonferrous Metal Soc. China*, 2007, **17**, 318-325.
11 S.V. Lamaka, M. L. Zheludkevich and K. A. Yasakau: *Electrochim. Acta*, 2007, **52**, 7231-7247.
12 G. Achary, H. P. Sachin, Y. A. Naik: *Mater. Chem. Phys.*, 2008, **107**, 44-50.
13 A. Popova, M. Christov and A. Vasilev: *Corros. Sci.*, 2011, **53**, 1770-1777.
14 M. K. Pavithra, T. V. Venkatesha and K. Vathsala: *Corros. Sci.*, 2010, **52**, 3811-3819.
15 X. Wang, H. Yang and F. Wang: *Corros. Sci.*, 2012, **55**, 145-152.
16 P. C. Okafar and Y. Zheng: *Corros. Sci.*, 2009, **51**, 850-859.
17 S. A. Umoren and E. E. Ebenso: *Mater. Chem. Phys.*, 2007, **106**, 387-393.
18 M. Bouklah, B. Hammouti, and A. Aouniti: *Appl. Surf. Sci.*, 2006, **252**, 6236-6242.
19 S. A. Umoren, O. Ogbobe and I. O. Igwe: *Corros. Sci.*, 2008, **50**, 1998-2006.
20 S. A. Umoren, Y. Li and F. H. Wang: *Corros. Sci.*, 2010, **52**, 1777-1786.
21 L.G. Qiu, Y. Wu and Y. M. Wang: *Corros. Sci.*, 2008, **50**, 576-582.
22 E. E. Oguzie, Y. Li and F. H. Wang: *Electrochim. Acta*, 2007, **52**, 6966-6988.
23 E. E. Oguzie, Y. Li and F. H. Wang: *J. Colloid Interface Sci.*, 2007, **310**, 90-98.
24 C. Jeyaprabha, S. Sathiyanarayanan, and G. Venkatachari: *Electrochim. Acta* 2006, **51**, 4080-4088.
25 X. M. Li, L. B. Tang and H. C. Liu: *Mater. Lett.*, 2008, **62**, 2321-2324.
26 A. Khamis, M. M. Saleh and M. I. Awad: *Corros. Sci.*, 2013, **66**, 343-349.
27 F. Diaba, C. L. Houerou and M. Grignon-Dubois: *J. Org. Chem.*, **2000**, **65**, 907-910.
28 F. M. Moghaddam, Z. Mirjafary and H. Saeidian: *Tetrahedron*, 2010, **66**, 3678-3681.
29 Z. Tao, S. Zhang and W. Li: *Corros. Sci.*, 2009, **51**, 2588-2595.
30 X. H. Li, S. D. Deng and G. N. Mu: *Corros. Sci.*, 2008, **50**, 420-430.
31 M. Sahin, S. Bilgic and H. Yılmaz: *Appl. Surf. Sci.*, 2002, **195**, 1-7.
32 K.F. Khaled and N. Hackenman: *Electrochim. Acta*, 2004, **49**, 485-495.
33 H. Keles, M. Keles and I. Dehri: *Colloids Surf. A*, 2008, **320**, 138-145.
34 M. Bouklah, B. Hammouti and A. Aouniti: *Appl. Surf. Sci.*, 2006, **252**, 6236-6242.
35 T. P. Hoar and R. P. Khera: *Proceedings 1st Europ Symp. on corrosion inhibitors,* Ferrara, Italy, 1960. 73.
36 R. Solmaz, E. Altunbas and G. Kardas: *Mater. Chem. Phys.*, 2011, **125**, 796-801.
37 A. Chetouani, A. Aouniti and B. Hammouti: *Corros. Sci.*, 2003, **45**, 1675-1684.
38 M. Behpour, S. M. Ghoreishi and N. Soltani: *Corros. Sci.*, 2009, **51**, 1073-1082.
39 R. Solmaz: *Corros. Sci.*, 2010, **52**, 3321-3330.
40 M. A. Veloz and I. González: *Electrochim. Acta*, 2002, **48**, 135-144.
41 A. R. S. Priya; V. S. Muralidharam and A. Subramania: *Corrosion*, 2008, **64**, 541-552.
42 P. Bommersbach, C. Alemany-Dumont and J. P. Millet: *Electrochim. Acta*, 2006, **51**, 4011-4018.
43 Q. Qu, Z. Z. Hao and L. Li *Corros. Sci.*, 2009, **51**, 569-574.
44 M. Lagrenée, B. Mernari, and M. Bouanis *Corros. Sci.*, 2002, **44**, 573-588.
45 G. Trabanelli, *Corrosion Inhibitors, in: F. Mansfeld (Ed.), Corrosion Mechanism;* Mercel Dekker: New York, 1987.
46 F. Bentiss, M. Traisnel and M. Lagrenee: *Corros. Sci.*, 2000, **42**, 127-146.
47 A. Y. Musa, A. A. H. Kadhum and A. B. Mohamad: *Corros. Sci.*, 2010, **52**, 526-533.
48 G. Quartarone, L. Ronchin, and A. Vavasori: *Corros. Sci.*, 2012, **64**, 82-89.
49 M. A. Hegazy, A. M. Badawi and S. S. Abd El Rehim, *Corros. Sci.*, in press.
50 S. Rengamani, S. Muralidharan and M. Anbu Kulandainathan: *J. Appl. Electrochem.*, 1994, **24**, 355-360.
51 J. O. M. Bockris and B. Yang: *J. Elecrochem. Soc.*, 1991, **138**, 2237-2252.
52 R. M. Tennet: *Science Data Book*; Oliver and Boyd: Edinburgh, 1978.
53 R. Fuchs-Godec and M. G. Pavlović: *Corros. Sci.*, 2012, **58**, 192-201.
54 N. Çalışkan and S. Bilgiç: *Appl. Surf. Sci.*, 2000, **153**, 128-133.
55 Y. Feng, K.S. Siow and W. K. Teo: *Corros. Sci.*, 1999, **41**, 829-852.
56 M. M. Saleh: *Mater. Chem. Phys.*, 2006, **98**, 83-89.
57 T. P. Hoar and R. D. Holliday: *J. Appl. Chem.* 1953, **3**, 502-513.
58 L. O. Riggs Jr and T. J. Hurd: *Corrosion*, 1967, **23**, 252-258.
59 G. M. Schmid and H. J. Huang: *Corros. Sci.*, 1980, **20**, 1041-1057.
60 P. N. Clark, E. Jackson and M. Robinson *Br. Corros. J.*, 1979, **14,** 33-39.
61 M. Abdallah, *Corros. Sci.*, 2002, **44**, 717-728.
62 J. de Damborenea, J. M. Bastidas and A. J. Vazquez: *Electrochim. Acta*, 1997, **42**, 455-459.
63 S. K. Shukla and M. A. Quraishi: *Corros. Sci.*, 2009, **51**, 1990-1997.
64 X. H. Li and G. N. Mu: *Appl. Surf. Sci.*, 2005, **252**, 1254-1265.
65 J. Marsh: *Advanced Organic Chemistry*; Wiley Eastern: New Delhi, 1988.
66 S. Martinez and I. Stern: *Appl. Surf. Sci.*, 2002, **199**, 83-89.
67 R. Fuchs-Godec: *Acta Chim. Slov.*, 2007, **54**, 492-502.
68 E.Cano, J. L. Polo and A. La: *Adsorption* 2004, **10**, 219-225.

69 F. Bentiss, M. Lebrini and M. Lagrenée: *Corros. Sci.*, 2005, **47**, 2915-2931.
70 N. Hackerman, E. S. Snavely and J. S. Payne: *J. Electrochem. Soc.*, 1966, **113**, 677-681.
71 N. Hackerman and A. C. Makrides *J. Phys. Chem.*, 1955, **59**, 707-710.
72 F. Bentiss, M. Lebrini, and M. Traisnel: *J. Appl. Electrochem.*, 2009, **39**, 1399-1407.
73 T. Murakawa and N. Hackerman: *Corros. Sci.*, **1964**, *4*, 387-396.
74 K. Shimizu, A. Shchukarev, P. A. Kozin, and J.-F. Boily: *Langmuir*, **2013**, *29*, 2623-2630.